Original Article
J. Korean Wood Sci. Technol. 2025, 53(4): 401-412
https://doi.org/10.5658/WOOD.2025.53.4.401

Journal of the Korean Wood Science and Technology
pISSN: 1017-0715 eISSN: 2233-7180
http://www.woodj.org

Preparation and Characterization of Demethylated Lignin for Efficient Palladium Adsorption

Dawoon SEO[1] ・ Sungwook WON[1] ・ Seon-Gyeong KIM[1] ・ Chaeeun KIM[1] ・ Hyoseung LIM[1] ・
Seojin KIM[1] ・ In-Gyu CHOI[1,2] ・ Hyo Won KWAK[1,2,†]

ABSTRACT

In this study, the preparation and characterization of demethylated kraft lignin (DKL), as a sustainable palladium (Pd) adsorbent, was studied. Demethylation was performed under acidic concentrated lithium bromide conditions, resulting in substitution of the methoxy groups with phenolic hydroxyl groups. Fourier-transform infrared and phosphorus-31 nuclear magnetic resonance analyses confirmed an increase in the phenolic hydroxyl content, whereas a concurrent decrease in the aliphatic OH content was observed due to acid-catalyzed elimination. Gel permeation chromatography results revealed a substantial increase in the molecular weight and polydispersity index, indicating condensation during the demethylation process. The increased molecular weight contributed to enhanced stability of the DKL in aqueous environments, with solubility less than 3% under acidic conditions. Furthermore, a zeta potential analysis showed that DKL exhibited a positive surface charge at pH 2, which enabled electrostatic interactions with $PdCl_4^{2-}$. DKL demonstrated a significantly higher Pd adsorption capacity (42.2 mg/g) than KL (4.5 mg/g). These findings suggest that demethylation is an effective strategy for enhancing the functionality of lignin and that DKL can serve as an eco-friendly and efficient biomass-based adsorbent for Pd recovery from acidic wastewater.

Keywords: lignin, demethylation, palladium, adsorption

1. INTRODUCTION

Palladium (Pd) is an exceptionally rare element, found only in limited regions of the world—such as South Africa, Russia, and Ontario, Canada—where it occurs at concentrations as low as 0.1 to 3 ng/g in the crust of the Earth (Liu *et al.*, 2024). Extensive industrial Pd use has led to an increase in the generation of Pd-containing wastewater. Without appropriate treatment, this waste poses a significant risk of environmental contamination. Therefore, the recovery of Pd from industrial effluents is vital for reclaiming this valuable resource and mitigating environmental pollution.

In parallel with these environmental concerns, Pd is also a critical platinum-group metal (PGM) with a high industrial demand, particularly for semiconductor inspection equipment, automotive catalytic converters, petroleum-refining catalysts, and fuel cell vehicles (Das and

---

Date Received March 14, 2025; Date Revised April 3, 2025; Date Accepted May 9, 2025; Published July 25, 2025

[1] Department of Agriculture, Forestry and Bioresources, College of Agriculture & Life Sciences, Seoul National University, Seoul 08826, Korea

[2] Research Institute of Agriculture and Life Sciences, Seoul National University, Seoul 08826, Korea

[†] Corresponding author: Hyo Won KWAK (e-mail: bk0502@snu.ac.kr, https://orcid.org/0000-0003-1630-7210)

Linert, 2016; Ohmatsu *et al.*, 2012; Yamada *et al.*, 2015). For example, Pd alloy materials are primarily used in pogo pins for test sockets during semiconductor production inspection processes (Tseng *et al.*, 2024). Various processing techniques have been employed in plunger manufacturing to achieve a low electrical resistivity, high flexibility, and broad range of hardness values. During the manufacturing process, a significant amount of Pd alloy scrap is generated as a byproduct, and this is typically classified as melting scrap and processing scrap (Yamada *et al.*, 2023). Therefore, recovering Pd from the by-product scrap generated in the plunger manufacturing process for pogo pins presents a valuable opportunity (Hammadi *et al.*, 2017).

Conventional Pd recovery methods include hydrometallurgy (Quinet *et al.*, 2005), ion exchange (Nikoloski *et al.*, 2015), solvent extraction (Paiva, 2017), and chemical precipitation (Yousif, 2019). However, these methods have disadvantages, such as high chemical consumption, secondary contamination, and low selectivity for Pd recovery. In contrast, adsorption offers advantages such as process simplicity, sustainability through repeated adsorption and desorption, and minimal secondary byproduct generation (Veglio and Beolchini, 1997; Wang *et al.*, 2015).

Lignin, a major component of green biomass, is the second most abundant natural polymer after cellulose (Bang *et al.*, 2022). Owing to its complex chemical network, lignin has traditionally been utilized as an energy source (Park *et al.*, 2020). Recently, its applicability has expanded to include use as a carbon material precursor (Lee *et al.*, 2021), emulsifier (Gao *et al.*, 2022), functional additive in cosmetics (Antunes *et al.*, 2023), adhesive filler (Yang *et al.*, 2019), UV-blocking film (Zheng *et al.*, 2023), food packaging material (Zubair *et al.*, 2024), and bio-based polyol for polyurethane production (Won *et al.*, 2024). In addition, lignin has been extensively investigated as an adsorbent material because of its diverse functional groups, including phenolic, aliphatic, and carboxyl groups (Kim *et al.*, 2023). However, the composition of lignin monomers, such as sinapyl alcohol (S), p-coumaryl alcohol (H), and coniferyl alcohol (G), varies significantly depending on the tree species and growth conditions (Park *et al.*, 2018). Notably, the methoxy groups adjacent to the phenolic hydroxyl groups contribute to cellulose fiber bonding but also hinder adsorption interactions between lignin and contaminants (Yunus *et al.*, 2024).

In this study, we investigated the effects of methoxy group substitution with hydroxyl groups on Pd adsorption after lignin demethylation. Structural modifications induced by demethylation were analyzed via Fourier-transform infrared (FTIR) and phosphorus-31 nuclear magnetic resonance (^{31}P NMR) spectroscopy. Furthermore, adsorption experiments were conducted to evaluate the effect of increasing the hydroxyl content on Pd–lignin interactions. Based on these findings, enhancing lignin hydroxyl functionality, via demethylation, could be proposed as a fundamental strategy for improving adsorption efficiency, not only for Pd recovery, but also for the removal of various waterborne contaminants.

2. MATERIALS and METHODS

2.1. Materials

Hardwood kraft lignin (KL), lithium bromide (LiBr, 99%), hydrobromic acid (HBr, Extra pure, 47% to 49%), palladium (II) chloride ($PdCl_2$, 99%), hydrochloric acid (HCl, ACS grade, 36.5% to 38.0%), and sodium hydroxide (NaOH, Extra pure), pH 2 buffer solution, were used. All chemicals were used without further purification, and distilled water was used throughout the study.

2.2. Preparation of demethylated kraft lignin

Demethylated kraft lignin (DKL) was prepared using an acidic concentrated lithium bromide (ACLB) system, and the 61% LiBr aqueous solution was prepared by mixing 24.4 g of LiBr and 15.6 g with distilled water. Moreover, 1 g of KL was added to a 61% LiBr aqueous solution and stirred, and then, 4 mL of 48% HBr was added. The solution was allowed to react in a small reactor in an oil bath at 120℃ for 30 min. After the reaction, filtration and washing were performed with distilled water, and the solution was dried in an oven at 60℃ to obtain the DKL.

2.3. Preparation of palladium model solution

$PdCl_2$ (50 mg) was added to a solution of 4 mL of 36% HCl and 16 mL of distilled water and completely dissolved. Additionally, 80 mL of distilled water was added to this solution to prepare a 500 ppm $PdCl_2$ aqueous solution. The pH was set to 2 using a pH meter and an aqueous NaOH solution. Using a pH 2 buffer solution, Pd aqueous solutions with concentrations of 200 ppm (the concentration of Pd, not the concentration of $PdCl_2$) were prepared.

2.4. Characterization of kraft lignin and demethylated kraft lignin

The chemical structures of KL and DKL were analyzed through FTIR (Summit, Thermo Fisher Scientific, Waltham, MA, USA) and ^{31}P NMR (Advance 600 MHz high-resolution spectrometers, Bruker, Berlin, Germany). FTIR analysis was performed in Attenuated Total Internal Reflection mode, and the range of 4,000–525 cm^{-1} was measured at a 4 cm^{-1} resolution with 64 scans. ^{31}P NMR analysis was performed to analyze the distribution and content of hydroxyl groups in the lignin. To this end, 40 mg of KL and DKL was dissolved in 0.5 mL of a mixture of anhydrous pyridine and chloroform-d (Deuterated Chloroform, $CDCl_3$), and 0.2 mL of a standard reagent (e-NHI, N-hydroxy-5norborene-2, 3-diimide) was added. The sample was prepared by mixing with 0.05 mL of a stabilizer [chromium (III) acetylacetonate solution] and then phosphate treatment with 0.1 mL of a phosphoric acid chloride reagent (2-chloro-4,4,5,5-tetramethyl-1,3,2-dioxaphospholane, TMDP).

Gel permeation chromatography (GPC, LC-40, Shimadzu, Kyoto, Japan) was performed to measure the molecular weight of the lignin. Each sample was dissolved in tetrahydrofuran at 1 mg/mL, filtered through a 0.45 μm polytetrafluoroethylene syringe filter (Advantech, Tokyo, Japan), and analyzed at a flow rate of 1 mL/min. GPC calibration was performed using ReadyCal Kit Poly (styrene) low (PSS Polymer Standards Service, Mainz, Germany), and the number-average molecular weight (Mn), weight-average molecular weight (Mw), and polydispersity index (PDI) of the lignin samples were calculated.

The surface charges of the lignin samples were investigated using a Zetasizer (Litesizer 500, Malvern, UK), depending on the pH of the solution. To measure water solubility, 1 g of each lignin sample was immersed in 30 mL of aqueous solutions of pH 2, 7, and 10 and stirred at 25℃ for 1 day. Subsequently, the undissolved samples were separated via centrifugation for 10 min at 6,800×g. Undissolved samples were dried in an oven at 60℃ for 12 h.

2.5. Palladium adsorption experiments

First, 10 mg of the lignin sample was added to 10 mL of a 200 ppm Pd aqueous solution, and adsorption experiments were performed at 25℃ for 30 min with stirring at 180 rpm. The concentration of Pd before and after all adsorption experiments was measured via inductively coupled plasma-atomic emission spectroscopy (ICP-AES, ICP5800, Agilent, Santa Clara, CA, USA). The Pd adsorption capacity of the lignin was calculated using the following Equation (1):

$$q_e = \frac{(C_0 - C_e) \times V}{M} \tag{1}$$

Where C_0 and C_e are the initial and equilibrium concentrations of the aqueous Pd solution (mg/L), respectively. V denotes the volume (l) of the Pd aqueous solution and M is the mass (g) of the lignin-based adsorbent. The atomic elements and chemical functional groups on the surfaces of the lignin samples before and after Pd adsorption were analyzed using X-ray photoelectron spectroscopy (XPS, AXIS SUPRA, Kratos, Manchester, UK).

3. RESULTS and DISCUSSION

Based on the FTIR analysis results for KL and DKL, it was predicted that the phenolic hydroxyl groups of lignin were increased through demethylation (Fig. 1). A peak at 1,710 cm^{-1}, corresponding to the carbonyl group, was observed for KL and DKL (Hwang *et al.*, 2021). In the case of KL, it showed distinct peaks at 3,500–3,200 cm^{-1} attributed to hydroxyl groups and 1,600 cm^{-1} due to the C = C bond of the aromatic ring (Watumlawar, 2023). In addition, it showed characteristic peaks at 1,120 cm^{-1} and 1,030 cm^{-1} owing to the C-H bond of the methoxy group (Lee *et al.*, 2019). However, for DKL that underwent demethylation, a significant decrease in the intensities of the peaks at 1,120 and 1,030 cm^{-1} was observed, which showed a decrease in the methoxy structure (Demuner *et al.*, 2024; Fiţigău *et al.*, 2013). In addition, compared to that with KL, the intensity of the peak at 3,500–3,200 cm^{-1} corresponding to the hydroxyl groups increased with DKL, confirming that the formation of hydroxyl groups increased through the demethylation process. Additionally, the FTIR peak at approximately 1,375 cm^{-1} for DKL indicates an increase in phenolic OH compared to that with KL (Pandey, 1999).

The hydroxyl content of the lignin before and after demethylation was calculated using ^{31}P NMR spectroscopy, and the results are presented in Fig. 2 and Table 1. KL and DKL showed chemical shifts and intensity changes in both the phenolic and aliphatic OH regions in the ^{31}P NMR spectra. For aromatic hydroxyl groups,

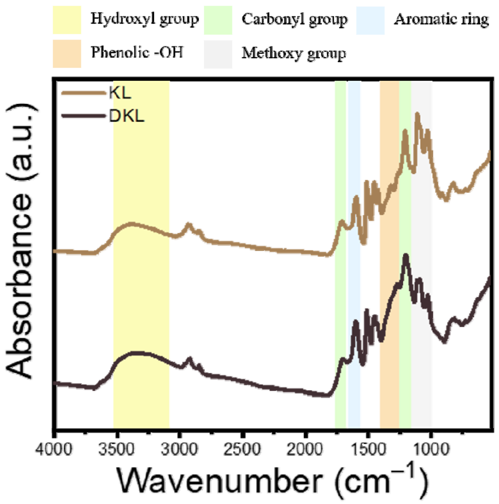

Fig. 1. Fourier-transform infrared spectra of kraft lignin (KL) and demethylated kraft lignin (DKL).

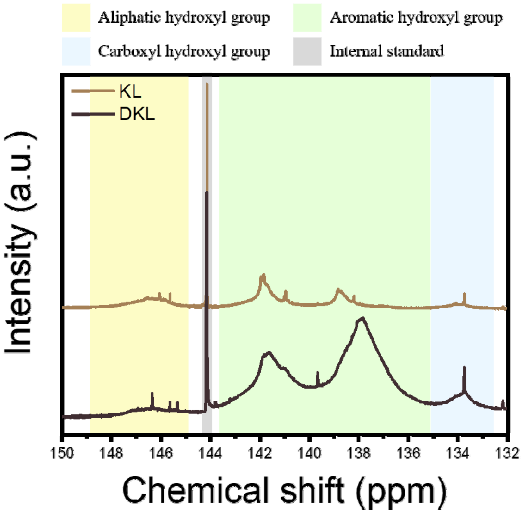

Fig. 2. Phosphorus-31 nuclear magnetic resonance spectra of kraft lignin (KL) and demethylated kraft lignin (DKL).

Table. 1. Quantitative phosphorus-31 nuclear magnetic resonance results of kraft lignin (KL) and demethylated kraft lignin (DKL)

	Aliphatic hydroxyl group (mmol/g)	Aromatic hydroxyl group (mmol/g)	Carboxyl hydroxyl group (mmol/g)	Total (mmol/g)
KL	0.98	2.43	0.18	3.58
DKL	0.31	7.11	0.83	8.25

the rapid increase in the aromatic hydroxyl content in DKL, from 2.43 mmol/g to 7.11 mmol/g, was attributed to demethylation of the methoxy groups in the ACLB system via S_N2 nucleophilic substitution, in which bromide ions cleave the ether bonds (Li *et al.*, 2020). Moreover, methyl-O-aryl ether linkages, such as α-O-4, β-O-4, and α-O-γ, were also cleaved in the ACLB system, leading to the formation of new phenolic hydroxyl groups (Li *et al.*, 2018). However, in the case of aliphatic hydroxyl groups, this decreased from 0.98 mmol/g to 0.31 mmol/g. The loss of aliphatic hydroxyl groups presumably resulted from the acid-catalyzed elimination of the aliphatic hydroxyl groups, and the primary hydroxy group was brominated in the ACLB system (Tao *et al.*, 2016; Wang *et al.*, 2023).

In general, the stability of lignin in an aqueous environment is vulnerable to alkaline conditions and is greatly affected by its molecular weight and hydroxyl group content (Evstigneev, 2011). GPC analysis was performed to observe the change in the molecular weight of lignin due to the demethylation process, and the results are shown in Fig. 3. Fig. 3(a) and (b) present the GPC results for KL and DKL, showing the molecular weight, PDI, and molecular weight distribution. For DKL, a peak was observed at a shorter retention time than that for KL, indicating that condensation occurred during demethylation [Fig. 3(c)]. As shown in Table 2, the Mn values for KL and DKL were 649 and 947 Da, respectively, the Mw values were 2,116 and 5,784 Da, respectively, and the PDI values were 3.26 and 6.11, respectively, indicating that condensation occurred in DKL. Li *et al.* (2020) reported that the demethylation of lignin is carried out in ACLB systems and that elevated temperatures promote lignin repolymerization through acid-induced condensation reactions, such as those between aromatic C5 or C6 positions and benzyl cations (Li *et al.*, 2020). This increase in the molecular weight due to condensation during demethylation also greatly affects the solubility of DKL. As shown in Fig. 3(d), KL exhibited solubilities of 18% and 29% at pH 2 and 7, respectively, which means that lignin was eluted when used as a water treatment material. Meanwhile, in the case of demethylated DKL, the stability in the aqueous environment increased owing to the effect of an increasing molecular weight, despite the increase in the hydroxyl group content. As a result, it showed a low solubility of less than 3% under both pH 2 and 7 conditions. This indicates that it can be used as a sustainable adsorption material under both acidic and neutral conditions for water treatment purposes.

When utilizing lignin as a heavy metal adsorption material, not only the content of hydroxyl groups but also the structural stability in various pH environments are important characteristics (Kim *et al.*, 2024). To examine the changes in surface charge characteristics resulting from lignin demethylation, the zeta potential was measured, and the results are shown in Fig. 4(a). For KL, negative charges of −18.2 mV at an acidic pH of 2 and −41.5 mV under pH 7 conditions were detected. This negative charge characteristic is because the hydroxyl and carbonyl groups present in lignin are the sites that mainly show charge characteristics (Chipman,

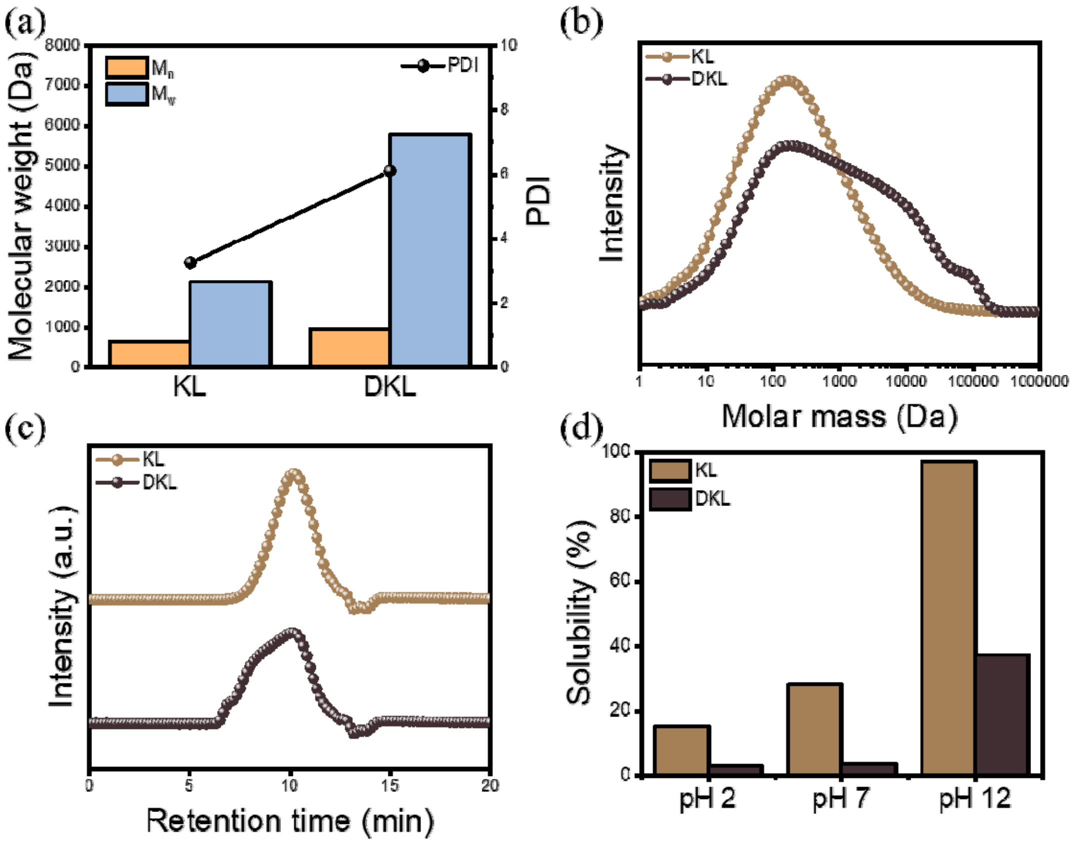

Fig. 3. Molecular weight characteristics and pH-dependent solubility of kraft lignin (KL) and demethylated kraft lignin (DKL). (a) Molecular weight (Mn, Mw) and polydispersity index (PDI), (b) molar mass distribution, (c) retention time distribution of KL and DKL, and (d) their solubility at pH 2, 7, and 10.

Table. 2. Number-average molecular weight (M_n), weight-average molecular weight (M_w), and polydispersity index (PDI) of kraft lignin (KL) and demethylated kraft lignin (DKL)

	M_n (Da)	M_w (Da)	PDI
KL	649	2,116	3.26
DKL	947	5,784	6.11

1986; Wiberg, 1999). However, for DKL, with an increased phenolic hydroxyl group content, a value of +5.3 mV was detected at pH 2, indicating that it can show positive charge characteristics under acidic conditions (Zhu *et al.*, 2024). Meanwhile, a value of −56.4 mV was detected at pH 7, which occurred because demethylation introduces more hydroxyl groups into the lignin molecular backbone, causing strong deprotonation and protonation [Fig. 4(b)]. Therefore, since DKL can have a positive surface charge under acidic conditions, such as at pH 2, unlike KL, it is expected that the electrostatic attraction-based adsorption of negatively charged contaminants will be possible.

In general, in the metal industry, including pogo pins for semiconductor inspection, Pd scrubs can be obtained by leaching with strong acids, such as sulfuric acid and

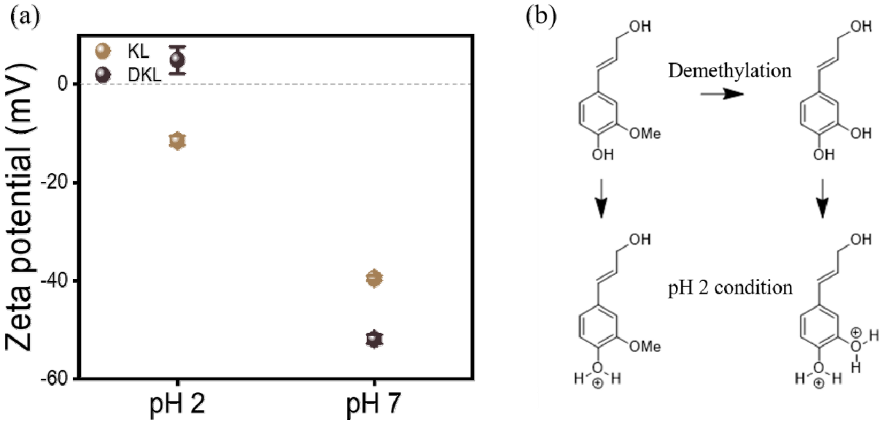

Fig. 4. Surface charge and ionization state of kraft lignin (KL) and demethylated kraft lignin (DKL) under acidic conditions. (a) Zeta potential and (b) ionization state under pH 2 conditions of KL and DKL.

hydrochloric acid, to obtain waste liquid. Therefore, a model Pd solution was prepared by dissolving $PdCl_2$ in a solution of hydrochloric acid at pH 2. As shown in Fig. 5(a), the $PdCl_2$ solution had an intense yellow color when prepared at 200 ppm, which is a phenomenon that occurs when Pd compounds are dissolved. KL and DKL were added to the Pd solution for the adsorption experiments. When KL was added, the color reduction of the Pd solution before and after adsorption was not significant, indicating that considerable Pd adsorption was not evident, even to the naked eye. However, when DKL was added, the yellow color of the Pd solution after adsorption was lighter and more transparent than that before adsorption, which indirectly indicates that significant adsorption had occurred.

To examine the actual Pd adsorption capacity, the Pd concentrations before and after adsorption were analyzed using ICP-AES [Fig. 5(b)]. The calculated Pd adsorption capacity of DKL was significantly higher than that of KL, at 42.2 mg/g compared to 4.5 mg/g, respectively. This excellent Pd adsorption capacity was also consistent with the color fading, visible to the naked eye, after adsorption. This phenomenon is attributed to the surface positive charge tendency of DKL under acidic condi-

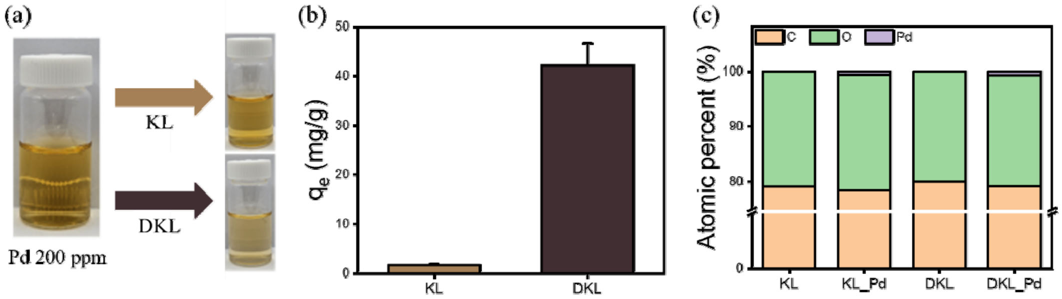

Fig. 5. Optical appearance, palladium (Pd) adsorption capacity, and surface atomic composition of kraft lignin (KL) and demethylated kraft lignin (DKL). (a) Optical images, (b) Pd adsorption capacity and (c) the atomic composition of KL and DKL.

tions, which is caused by an increase in the phenolic hydroxyl groups in the demethylation process, strengthening the electrostatic attraction with $PdCl_4^{2-}$ and enabling the recovery of a larger amount of the Pd compound (Zhu *et al.*, 2024). The Pd contents of KL and DKL, which were confirmed through elemental composition analysis obtained from the actual XPS full spectrum [Fig. 5(c)], also showed a higher Pd content in DKL, indicating that Pd was adsorbed on the surface of DKL.

To understand the Pd adsorption behavior of DKL, XPS was performed on the adsorbent surface before and after adsorption, and the high-resolution XPS spectrum in the Pd detection region of 345–335 eV is shown in Fig. 6. For DKL, before adsorption, no noticeable Pd peak was detected in the range of 335–345 eV [Fig. 6(a) and (c)]. However, after adsorption, a distinct Pd 3d peak appeared, indicating that the Pd compounds were successfully adsorbed onto the DKL surface [Fig. 6(b) and (d)]. In particular, as shown in Fig. 6(d), the Pd $3d_{5/2}$ and Pd $3d_{3/2}$ XPS spectra showed strong intensities at 343.0 eV and 337.8 eV, respectively; these are typical characteristics of Pd(II) and are consistent with the results when it exists as $PdCl_4^{2-}$ (Savastano *et al.*, 2019). In addition, the fact that the characteristic peaks of Pd(0) at 345.0 eV and 340.5 eV were not detected indicates that the reduction of Pd adsorbed on the surface

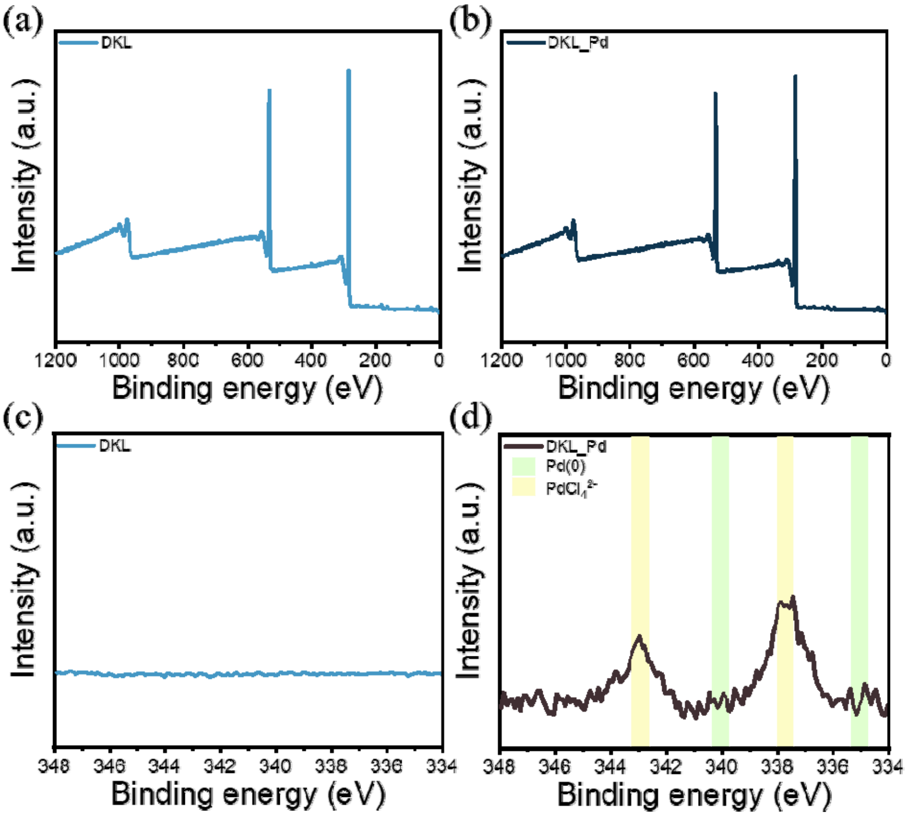

Fig. 6. X-ray photoelectron spectroscopy (XPS) spectra of demethylated kraft lignin (DKL) before and after palladium (Pd) adsorption: (a) survey spectrum and (c) high-resolution Pd 3d spectrum before adsorption; (b) survey spectrum and (d) high-resolution Pd 3d spectrum after adsorption.

of DKL did not occur (Karhu *et al.*, 2003). This indicates that electrostatic interactions between the surface of DKL and $PdCl_4^{2-}$ could be the main adsorption mechanism (Zhu *et al.*, 2024). Kim *et al.* (2024) reported that in the case of lignin modified via cationization using polyethyleneimine, the surface was enriched with amine groups, which increased the electrostatic interaction with the anionic Pd compound (Kim *et al.*, 2024).

4. CONCLUSIONS

In this study, we investigated the possibility of using lignin as an eco-friendly adsorbent to recover Pd from Pd-scrub wastewater generated at industrial sites. For this purpose, the demethylation of KL was performed under ACLB conditions. For the obtained DKL, the content of aromatic hydroxyl groups increased by approximately 190%, and at the same time, the molecular weight increased owing to repolymerization, which resulted in excellent stability in an aqueous environment. Unlike KL, DKL exhibited positive charge characteristics under acidic conditions (pH 2), which enabled electrostatic interactions with $PdCl_4^{2-}$. DKL showed excellent Pd adsorption capacity (42.2 mg/g) compared to KL (4.5 mg/g). In addition, it is expected that the Pd recovery efficiency can be maximized through additional chemical modification utilizing the increased phenolic hydroxyl groups of lignin as the main functional group. These results suggest that lignin can be utilized as a useful biomass-based adsorbent for the recovery of PGMs, including Pd, and that it also has the potential to be upcycled into a high-performance catalyst by reducing the amount of Pd adsorbed on the surface of lignin.

CONFLICT of INTEREST

No potential conflict of interest relevant to this article was reported.

ACKNOWLEDGMENT

This work was supported by the Technology Innovation Program (RS-2024-00437223, Development of 3N grade palladium alloy ingot manufacturing technology by directly utilizing scrap of plunger) funded by the Ministry of Trade, Industry & Energy (MOTIE, Korea). This work was supported by the ‘R&D Program for Forest Science Technology (RS-2024-00403384)’ funded by the Korea Forest Service (Korea Forestry Promotion Institute).

REFERENCES

Antunes, F., Mota, I.F., Fangueiro, J.F., Lopes, G., Pintado, M., Costa, P.S. 2023. From sugarcane to skin: Lignin as a multifunctional ingredient for cosmetic application. International Journal of Biological Macromolecules 234: 123592.

Bang, J., Kim, J., Kim, Y., Oh, J.K., Kwak, H.W. 2022. Preparation and characterization of hydrophobic coatings from carnauba wax/lignin blends. Journal of the Korean Wood Science and Technology 50(3): 149-158.

Chipman, D.M. 1986. Electron affinity of hydroxyl radical. The Journal of Chemical Physics 84(3): 1677-1682.

Das, P., Linert, W. 2016. Schiff base-derived homogeneous and heterogeneous palladium catalysts for the Suzuki–Miyaura reaction. Coordination Chemistry Reviews 311: 1-23.

Demuner, I.F., Borges Gomes, F.J., Coura, M.R., Demuner, A.J., Macedo Ladeira Carvalho, A.M., Cubides-Román, D.C., Ribas Batalha, L.A., Castro, R.N. 2024. Chemical modification of kraft lignin using black liquor heat treatment. Nordic Pulp & Paper Research Journal 39(3): 283-295.

Evstigneev, E.I. 2011. Factors affecting lignin solubility. Russian Journal of Applied Chemistry 84(6): 1040-

1045.

Fiţigău, I.F., Peter, F., Boeriu, C.G. 2013. Structural analysis of lignins from different sources. International Journal of Chemical, Molecular, Nuclear, Materials and Metallurgical Engineering 7(4): 167-172.

Gao, K., Liu, J., Li, X., Gojzewski, H., Sui, X., Vancso, G.J. 2022. Lignin nanoparticles as highly efficient, recyclable emulsifiers for enhanced oil recovery. ACS Sustainable Chemistry & Engineering 10(29): 9334-9344.

Hammadi, M.Q., Yassen, R.S., Abid, K.N. 2017. Recovery of platinum and palladium from scrap automotive catalytic converters. Al-Khwarizmi Engineering Journal 13(3): 131-141.

Hwang, U.T., Bae, J., Lee, T., Hwang, S.Y., Kim, J.C., Park, J., Choi, I.G., Kwak, H.W., Hwang, S.W., Yeo, H. 2021. Analysis of carbonization behavior of hydrochar produced by hydrothermal carbonization of lignin and development of a prediction model for carbonization degree using near-infrared spectroscopy. Journal of the Korean Wood Science and Technology 49(3): 213-225.

Karhu, H., Kalantar, A., Väyrynen, I.J., Salmi, T., Murzin, D.Y. 2003. XPS analysis of chlorine residues in supported Pt and Pd catalysts with low metal loading. Applied Catalysis A: General 247(2): 283-294.

Kim, J., Kim, Y., Jung, S., Yun, H., Won, S., Yeo, H., Choi, I.G., Kwak, H.W. 2024. Green lignocellulosic superadsorbent for superior Pd(II) removal and cascade catalytic conversion. Separation and Purification Technology 332: 125732.

Kim, J., Kim, Y., Jung, S., Yun, H., Yeo, H., Choi, I.G., Kwak, H.W. 2023. Cationized lignin loaded alginate beads for efficient Cr(VI) removal. Journal of the Korean Wood Science and Technology 51(5): 321-333.

Lee, H., Kim, S., Park, M.J. 2021. Specific surface area characteristic analysis of porous carbon prepared from lignin-polyacrylonitrile copolymer by activation conditions. Journal of the Korean Wood Science and Technology 49(4): 299-314.

Lee, H.W., Jeong, H., Ju, Y.M., Youe, W.J., Lee, J., Lee, S.M. 2019. Pyrolysis properties of lignins extracted from different biorefinery processes. Journal of the Korean Wood Science and Technology 47(4): 486-497.

Li, N., Li, Y., Yoo, C.G., Yang, X., Lin, X., Ralph, J., Pan, X. 2018. An uncondensed lignin depolymerized in the solid state and isolated from lignocellulosic biomass: A mechanistic study. Green Chemistry 20(18): 4224-4235.

Li, Z., Sutandar, E., Goihl, T., Zhang, X., Pan, X. 2020. Cleavage of ethers and demethylation of lignin in acidic concentrated lithium bromide (ACLB) solution. Green Chemistry 22(22): 7989-8001.

Liu, H., Wu, P., Wang, K., Li, Q., Yu, C., Li, X., Cai, Y., Feng, W., Yuan, L. (2024). Palladium recovery from acidic solution with phenanthroline-based covalent organic polymers as adsorbents for efficient heterogeneous catalysis. Green Chemistry 26(2): 804-814.

Nikoloski, A.N., Ang, K.L., Li, D. 2015. Recovery of platinum, palladium and rhodium from acidic chloride leach solution using ion exchange resins. Hydrometallurgy 152: 20-32.

Ohmatsu, K., Ito, M., Kunieda, T., Ooi, T. 2012. Ion-paired chiral ligands for asymmetric palladium catalysis. Nature Chemistry 4(6): 473-477.

Paiva, A.P. 2017. Recycling of palladium from spent catalysts using solvent extraction: Some critical points. Metals 7(11): 505.

Pandey, K.K. 1999. A study of chemical structure of soft and hardwood and wood polymers by FTIR spectroscopy. Journal of Applied Polymer Science 71(12): 1969-1975.

Park, S.Y., Choi, J.H., Cho, S.M., Choi, J.W., Choi, I.G.

2020. Structural analysis of open-column fractionation of peracetic acid-treated kraft lignin. Journal of the Korean Wood Science and Technology 48(6): 769-779.

Park, S.Y., Hong, C.Y., Kim, S.H., Choi, J.H., Lee, H.J., Choi, I.G. 2018. Studies on photoprotection of walnut veneer exposed to UV light. Journal of the Korean Wood Science and Technology 46(3): 221-230.

Quinet, P., Proost, J., Van Lierde, A. 2005. Recovery of precious metals from electronic scrap by hydrometallurgical processing routes. Mining, Metallurgy & Exploration 22: 17-22.

Savastano, M., Arranz-Mascarós, P., Clares, M.P., Cuesta, R., Godino-Salido, M.L., Guijarro, L., Gutiérrez-Valero, M.D., Inclán, M., Bianchi, A., García-España, E. 2019. A new heterogeneous catalyst obtained via supramolecular decoration of graphene with a Pd^{2+} azamacrocyclic complex. Molecules 24(15): 2714.

Tao, J., Hosseinaei, O., Delbeck, L., Kim, P., Harper, D.P., Bozell, J.J., Rials, T.G., Labbé, N. 2016. Effects of organosolv fractionation time on thermal and chemical properties of lignins. RSC Advances 6(82): 79228-79235.

Tseng, S.C., Lee, C.T., Chen, W.C., Tsai, H.Y. 2024. Effect of onion-like carbon on the resistance and adhesion of pogo pins with titanium adhesive layer of varying thicknesses. Surface and Coatings Technology 479: 130585.

Veglio, F., Beolchini, F. 1997. Removal of metals by biosorption: A review. Hydrometallurgy 44(3): 301-316.

Wang, J., Li, J., Wei, J. 2015. Adsorption characteristics of noble metal ions onto modified straw bearing amine and thiol groups. Journal of Materials Chemistry A 3(35): 18163-18170.

Wang, Y., Chen, M., Yang, Y., Ralph, J., Pan, X. 2023. Efficient *O*-demethylation of lignin-derived aromatic compounds under moderate conditions. RSC Advances 13(9): 5925-5932.

Watumlawar, E.C. 2023. Effects of precipitation pH of black liquor on characteristics of precipitated and acetone-fractionated kraft lignin. Journal of the Korean Wood Science and Technology 51(1): 38-48.

Wiberg, K.B. 1999. The interaction of carbonyl groups with substituents. Accounts of Chemical Research 32(11): 922-929.

Won, S., Bang, J., Park, S.W., Kim, J., Jung, M., Jung, S., Yun, H., Yeo, H., Choi, I.G., Kwak, H.W. 2024. Effect of ethanol fractionation of lignin on the physicochemical properties of lignin-based polyurethane film. Journal of the Korean Wood Science and Technology 52(3): 221-233.

Yamada, M., Gandhi, M.R., Kondo, Y., Haga, K., Shibayama, A., Hamada, F. 2015. Selective sorption of palladium by thiocarbamoyl-substituted thiacalix[n]arene derivatives immobilized on amberlite resin: Application to leach liquors of automotive catalysts. RSC Advances 5(74): 60506-60517.

Yamada, M., Ohira, T., Watanabe, N., Katagiri, H., Shibayama, A., Hamada, F. 2023. Recovery of Pd(II) by solvent extraction with a dithiophenol-based extractant from the undiluted leachate of spent automotive catalysts followed by water scrubbing and thiourea stripping. Hydrometallurgy 215: 105986.

Yang, I., Jeong, H., Lee, J.J., Lee, S.M. 2019. Relationship between lignin content and the durability of wood pellets fabricated using *Larix kaempferi* C. sawdust. Journal of the Korean Wood Science and Technology 47(1): 110-123.

Yousif, A.M. 2019. Recovery and then individual separation of platinum, palladium, and rhodium from spent car catalytic converters using hydrometallurgical technique followed by successive precipitation methods. Journal of Chemistry 2019(1): 2318157.

Yunus, R.M., Zeglam, T., Khan, M.M.R., Jemaat, Z., Othman, M.P. 2024. Recent methods of lignin demethylation: A mini review. AIP Conference Proceedings 3014: 070004.

Zheng, T., Yang, L., Zhang, X.F., Yao, J. 2023. Conversion of corncob residue to sustainable lignin/cellulose film with efficient ultraviolet-blocking property. Industrial Crops and Products 196: 116517.

Zhu, Q., Zhu, J., Huang, K. 2024. Selectivity of modified pomegranate peel for gold, platinum, and palladium: Adsorption behavior, mechanism, and recovery. Journal of Environmental Chemical Engineering 12(2): 111902.

Zubair, M., Rauf, Z., Fatima, S., Ullah, A. 2024. Lignin-derived bionanocomposites as functional food packaging materials. Sustainable Food Technology 2: 945-966.